Computer Physics Communications 63 (1991) 529–537
North-Holland

Efficient time propagation for finite-difference representations of the time-dependent Schrödinger equation

C. Cerjan and K.C. Kulander
Lawrence Livermore National Laboratory, Livermore, CA 94550, USA

Received 1 June 1990; in final form 11 June 1990

The applicability of the Chebyshev time propagation algorithm for the solution of the time-dependent Schrödinger equation is investigated within the context of differencing schemes for the representation of the spatial operators. Representative numerical tests for the harmonic oscillator and Morse potentials display the utility and limitations of this combined approach. Substantial increases in time step are possible for these lower-order methods compared with other propagators commonly used in differencing schemes, but if very high accuracy is desired for these cases difference methods remain less efficient computationally than the corresponding spectral spatial representation when both methods are applicable.

1. Introduction

The rapid expansion in computational power has fueled a broad range investigation into the efficiency of various algorithms for the solution of general classes of partial differential equations. Separate disciplines have quite different computational difficulties, but the features of some numerical treatments transcend their respective areas and find applicability to another set of problems. Many problems in atomic and molecular physics demand an explicit quantum mechanical treatment. The solution of the time-dependent nonrelativistic Schrödinger equation, which is fundamental to this investigation, has benefited greatly from the increases in computer memory and speed, and from the development of grid methods developed in other fields. Indeed, for some classes of problems the time-dependent methods have become competitive with the more developed time-independent treatments in the sense of quantitative accuracy. Time-dependent methods possess clear advantages for explicitly time-dependent Hamiltonian operators. Additionally, the correspondence with classical and semiclassical treatments is very natural and immediate with a time-evolved solution. As in other disciplines, the search for general and efficient computational methods lies at the center of much recent research.

Since the nonrelativistic Schrödinger equation is a parabolic equation, it resembles in form the standard diffusion equation. There is a significant physical difference, of course, since the solution diffuses in imaginary time and is not naturally dissipative; thus dispersion becomes a critical numerical issue. Both applications face a similar problem: a balanced approximation of the second-order spatial derivatives and first-order time derivative. Thus, some of the first grid methods adapted algorithms developed for the heat transfer equation [1]. In particular, the spatial operator was approximated by a low-order differencing form and the time propagation introduced by use of a "unitarized" approximation to the time evolution operator (the Crank–Nicolson form).

Later numerical treatments followed a different course – the spectral decomposition of the spatial operator combined with various time propagation techniques. The solution of the paraxial equation in optics, which is identical in form to the

Elsevier Science Publishers B.V. (North-Holland)

Schrödinger equation, led to the so-called "split-operator" algorithm which is a unitary approximation to the evolution operator [2], hence unconditionally stable like the Crank–Nicolson technique. A parallel approach was suggested from the numerical solution of the acoustic (Helmholtz) wave equation [3]. More precisely, in this work the power of the spectral method was recognized and coupled to a low-order, robust and inefficient time differencing scheme. This time evolution method is only conditionally stable, but is quite generally applicable to explicitly time-dependent potentials. The high-order accuracy of the spectral decomposition has generated much interest in the development of correspondingly accurate time evolution approximations. The development of the so-called "Chebyshev expansion" method [4] was proposed as such a high-order approximation. For a large class of physically interesting problems, this method provides an efficient and accurate treatment of the temporal representation.

The purpose of the research described below is to study the use of the Chebyshev expansion with a differencing scheme for the spatial operator. Since the expansion method permits large time stepping, the obvious point arises whether a lower-order scheme can be usefully extended. Current applications of the differencing method often rely on the Crank–Nicolson or related schemes [5]. A low-order differencing method is in principle faster than a spectral method since it scales as the "bandedness" times the size of the grid, $\mathcal{O}(bN)$, rather than as $\mathcal{O}(N \log N)$. The question of numerical efficiency immediately arises, though, in the balance between speed and accuracy. Preliminary investigations by the authors in the study of the photodissociation of CO_2 indicated that this would be a viable approach for the calculation of the necessary autocorrelation functions [6]. This question is addressed here by examining the error in the time-dependent wavefunction introduced by the low-order differencing approximation using several simple, representative examples. In the next section, section 2, the differencing scheme and the Chebyshev expansion method are briefly reviewed. Section 3 presents the numerical applications of this combined approach. Section 4 concludes the work with a summary of the results and a discussion of the limitations and extensions of this approach.

2. Mathematical background

One of the simplest and most robust means of approximating a spatial derivative is a local polynomial expansion of the unknown fuction. On a grid, this expansion has the form of a difference equation

$$\frac{\partial^2\psi(x_n)}{\partial x^2} \approx \frac{\psi(x_{n+1}) - 2\psi(x_n) + \psi(x_{n-1})}{(\Delta x)^2}, \quad (1)$$

where $\Delta x = x_{n+1} - x_n$ and $\psi(x)$ is the specified function. Since this approximation is valid to order $(\Delta x)^4$, a relatively inexpensive improvement can be simply obtained by using the next higher-order expansion, accurate to order $(\Delta x)^6$, so that the second-order spatial derivative becomes

$$\frac{\partial^2\psi(x_n)}{\partial x^2} \approx (\psi(x_{n+2}) - 16\psi(x_{n+1}) + 30\psi(x_n) - 16\psi(x_{n-1}) + \psi(x_{n-2}))\left[12(\Delta x)^2\right]^{-1}. \quad (2)$$

Of course this procedure could be straightforwardly extended leading to higher-order polynomial approximations. For most applications, eq. (2) represents a suitable balance between accuracy and computational speed. The accuracy and stability of various grid representations can often be more easily seen by decomposing the solution to the finite-difference equation in a Fourier series. The improvement in accuracy is reflected in the dispersion relation associated with this approximation for small step size

$$\frac{2\cos(2\theta) - 32\cos(\theta) + 30}{12(\Delta x)^2} = \frac{\theta^2 + \mathcal{O}(\theta^6)}{(\Delta x)^2}, \quad (3)$$

where $\theta = k\,\Delta x$ and k is the Fourier series variable conjugate to x. This dispersion relation is superior to that obtained from eq. (1)

$$\frac{2\cos(\theta) - 1}{(\Delta x)^2} = \frac{\theta^2 + \mathcal{O}(\theta^4)}{(\Delta x)^2}. \quad (4)$$

Thus the higher-order differencing formulae translate directly into polynomial corrections to the exact dispersion relation. This improvement should be contrasted with the spectral methods which have exponential improvement for approximately band-limited functions. Spectral methods replace direct calculation of the differentiation operator by using Fourier convolution. The Fourier transform of the wavefunction is obtained, multiplied by k^2 and then back-transformed to the original direct (co-ordinate) space. For localized functions, this procedure is *exact* at the nodal points.

The second important numerical concern is of course a treatment of the time propagation. For an operator, H, satisfying the linear equation

$$\frac{\mathrm{i}}{\hbar}\frac{\partial\psi(x,t)}{\partial t} = H\left(\frac{\partial}{\partial x}, x\right)\psi(x,t), \tag{5}$$

the formal solution to the time evolution of the function $\psi(x, t)$ is given by

$$\psi(x,t) = \exp\left(-\frac{\mathrm{i}}{\hbar}Ht\right)\psi(x,0). \tag{6}$$

The evolution operator can be efficiently expanded in a Fourier–Bessel series involving the operator and time

$$\exp\left(-\frac{\mathrm{i}}{\hbar}Ht\right) \approx \sum_{n=0}^{N} J_n(t)T_n\left(-\frac{\mathrm{i}}{\hbar}H\right), \tag{7}$$

where the J_n are Bessel functions of the first kind and the T_n are Chebyshev polynomials. The number of terms chosen in the summation, N, is dictated by the spectral range (the highest eigenvalue represented in the problem) and the desired time step in each interval, Δt. After specification of the energy span, by estimating the largest potential and kinetic energy on the grid, an error tolerance can be imposed for a given choice of Δt which specifies that the coefficients, $J_n(t)$, must be larger than this tolerance. In principle only one step could be taken, but this choice might practically force too many Hamilitonian operations. The Chebyshev polynomials satisfy a three-term recurrence relation which is very efficient numerically. The details of this propagation scheme have been discussed more fully in previous work [4].

The utility of the Chebyshev expansion arises from the large time steps that can be taken. The efficiency of the method generally increases with increasing time step since the additional operator evaluations required do not scale linearly with the change in time step. Previous applications of the Chebyshev expansion have relied on the high accuracy of the spectral method for the spatial representation of the derivative operator. By analogy to the spectral methods, differencing operators could display a corresponding enhancement in time propagation at a different level of accuracy. This possibility is investigated in the next section for a few simple, demonstrative cases.

3. Numerical applications

To test the combined differencing and Chebyshev expansion method, the time-dependent Schrödinger equation

$$\mathrm{i}\frac{\partial\psi(x,t)}{\partial t} = -\frac{\hbar^2}{2m}\frac{\partial^2\psi(x,t)}{\partial x^2} + V(x)\psi(x,t) \tag{8}$$

was solved for free-particle propagation and two different potential choices. The evolution of a particle in the absence of a potential is sufficiently simple so that the general features of the error analysis can be readily understood and the special but important examples of one-dimensional harmonic motion and potential scattering are useful as guides to more complicated and realistic simulations.

For the first case of free-particle motion, the initial wavepacket was chosen to be

$$\psi(x,0) = \exp(\mathrm{i}p_0x)\exp\left(-\frac{(x-x_0)^2}{\sigma^2}\right). \tag{9}$$

This wavepacket was then evolved by Chebyshev expansion using either the five-point differencing method of eq. (2) or the spectral method. The parameters chosen for this comparison are listed in table 1. Specifically, the number of spatial grid points was 512 for all calculations with a spacing of 0.5 bohr; the time interval was segmented into

Table 1
Free-particle numerical parameters (atomic units)

$N_{grid} = 512$	$x_0 = 0.0$	
$\Delta x = 0.5$	$\sigma = 10.0$	mass = 1.0
$\Delta t = 5.0$	$p_0 = 0.0, 0.5$	

steps of 5 atomic time units. An electron, atomic mass of 1, was selected as the evolving particle. These choices led to 183 Bessel expansion coefficients. In fig. 1 and 2, the logarithmic error in both the amplitude (fig. 1) and phase (fig. 2) of the evolving wavefunction is plotted as a function of time. The amplitude error is defined to be the deviation of the modulus of the inner product from unity

$$\epsilon_{amp} \equiv 1 - |(\psi_{exact}(x, t), \psi_{approx}(x, t))|, \qquad (10)$$

and the phase error, ϵ_{ph}, is the argument of the complex inner product.

More specifically, in fig. 1 the results of two runs using the differencing approximation are compared with one spectral representation run. In both cases, the Chebyshev error tolerance was set to 10^{-8} with the "exact" wavefunction given by a spectral solution with a tolerance of 10^{-14}. The

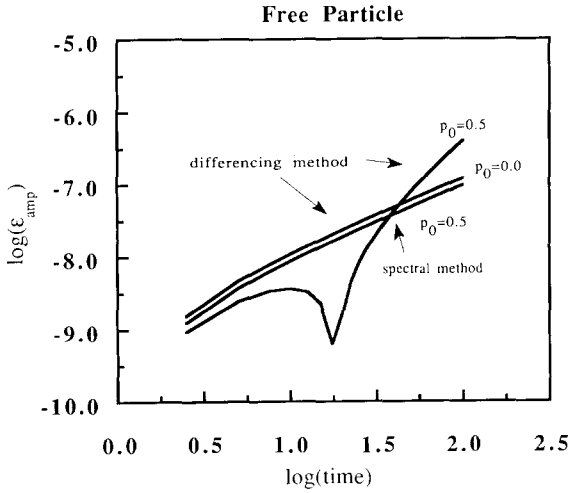

Fig. 1. The logarithm of the overlap amplitude error is plotted as a function of time for free-particle evolution. Results are presented for the Chebyshev expansion with either a finite-difference or spectral method.

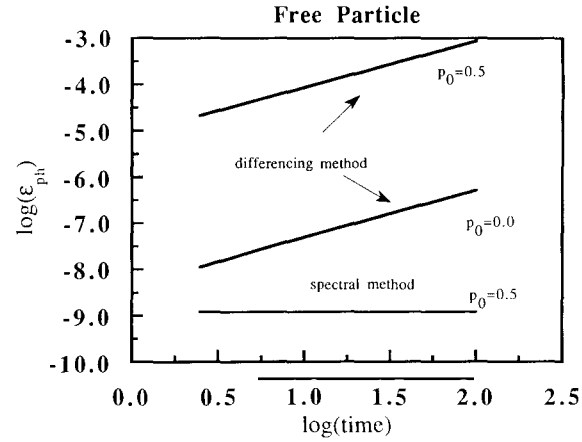

Fig. 2. The logarithm of the overlap phase error is plotted as a function of time for free-particle evolution. Both finite-difference and spectral method results are shown. The phase error dominates the overall error.

two possible sources of error in the calculated wavefunction are in the amplitude and phase. To investigate the sensitivity of the results to the overall phase (that is, when p_0 is not zero), the first differencing calculation used $p_0 = 0.0$ while the second used $p_0 = 0.50$. It is evident from fig. 1 that the amplitude error is small for either case and both calculations compare favorably to the spectral run. On the other hand, fig. 2 depicts the poor performance in phase accuracy that attends the differencing method, especially for nonzero initial phase.

This phase error can be understood from a more quantitative viewpoint. The free particle's propagation is given by

$$\psi(x, t) = \exp(-i\alpha t \nabla^2)\psi(x, 0), \qquad (11)$$

where $\alpha = \hbar^2/2m$. The different representations of the derivative operator provide the two numerical approximations

$$\psi_F(x, t) = \exp(-i\alpha t \nabla_F^2 \psi(x)), \qquad (12)$$

where ∇_F^2 is the Fourier convolution form mentioned above and

$$\psi_D(x, t) = \exp(-i\alpha t \nabla_D^2 \psi(x)), \qquad (13)$$

where ∇_D^2 is the polynomial (differencing) representation of the Laplace operator. The error integral in eq. (11) is

$$(\psi_F(x, t), \psi_D(x, t)) = (2R)^{-1}\int_{-R}^{R} \exp\left[i\alpha t\left(\nabla_F^2 - \nabla_D^2\right)\psi(x)\right] dx, \tag{14}$$

where R is the maximum spatial extent of the grid: $R = N_{grid}\Delta x/2$. If the function is localized on the grid, then the Fourier representation will be accurate to the accuracy of the computer, hence it can be chosen as the "exact" spatial representation in this error test. Consequently, the difference in Fourier representations can be evaluated using eq. (3)

$$\left(\nabla_F^2 - \nabla_D^2\right) \approx k^2 - \left[k^2 + \mathcal{O}\left(k^6(\Delta x)^4\right)\right] = ak^6(\Delta x)^4, \tag{15}$$

where a is a real constant. Thus the integrand in eq. (14) becomes

$$\exp\left(i\alpha t\left(\nabla_F^2 - \nabla_D^2\right)\psi(x)\right) \approx \exp\left[i\alpha a t(\Delta x)^4\psi^{(vi)}(x)\right], \tag{16}$$

where $\psi^{(vi)}(x)$ is the sixth derivative of the original wavefunction. The specific form chosen for the initial wavefunction in eq. (10) yields

$$\psi^{(vi)}(x) = \left(\sum_{n=0}^{6} b_n x^n\right)\psi(x) \equiv g(x)\psi(x). \tag{17}$$

In general, the coefficients b_n are complex and are real only if $p_0 = 0$. This special case provides the error expression

$$(\psi_F(x, t), \psi_D(x, t)) = \int_{-R}^{R} \exp\left[i\alpha t a(\Delta x)^4 g(x)\psi(x)\right] dx. \tag{18}$$

The intermediate value theorem implies that

$$(\psi_F(x, t), \psi_D(x, t)) = A \exp\left[i\alpha t a(\Delta x)^4 g(\xi)\psi(\xi)\right] \tag{19}$$

for some $\xi \in [-R, R]$.

Table 2
Harmonic oscillator numerical parameters (atomic units)

$N_{grid} = 512$	$x_0 = 0.0$	$\omega = 1.0$
$\Delta x = 0.1$	$\sigma = 1.0$	mass = 1.0
$\Delta t = 1.0$	$p_0 = 0.0$	

It is clear from an examination of this last expression that if $g(x)$ and $\psi(x)$ are real functions ($p_0 = 0$) then the error will only accumulate in the phase and not in the amplitude. Conversely, for $p_0 \neq 0$ the amplitude and phase will both display significant error accumulation controlled by the magnitude of p_0. Arguing by plausibility, more complicated circumstances will have the same qualitative behavior: predominant phase error which accumulates if the initial wavepacket has a complex component; significant error for the amplitude with an initial complex factor. Generalizing this conclusion slightly, it is thus worthwhile to minimize the initial phase for better error control.

As a second test, the evolution of an electron in a harmonic well, $V(x) = (\omega^2/2)x^2$, was followed using the initial wavefunction given in eq. (9) and calculational parameters listed in table 2. A direct comparison of grid efficiency was attempted in this case by decreasing the grid spacing used for the differencing operator. For the same grid choices, the finite-differencing scheme is of course faster than the spectral method. For example, for the harmonic oscillator test case the difference was a constant factor of about 4.6 over a wide choice of grid parameters. In other words, if the calculation requires about five times as many grid points using the difference formulae to achieve the desired accuracy, the computation times will be equivalent. The spectral method needs far fewer grid points for a given error tolerance than any high-order differencing scheme since differencing posseses polynomial convergence as opposed to exponential convergence for a band-limited spectral representation. Figure 3 contains the amplitude error comparison for the differencing approximation with three choices of grid spacing, 0.2, 0.1, and 0.05; the Chebyshev error tolerance was again set to 10^{-8}. A spectral calculation for a spacing of 0.5 is also plotted. In all cases the

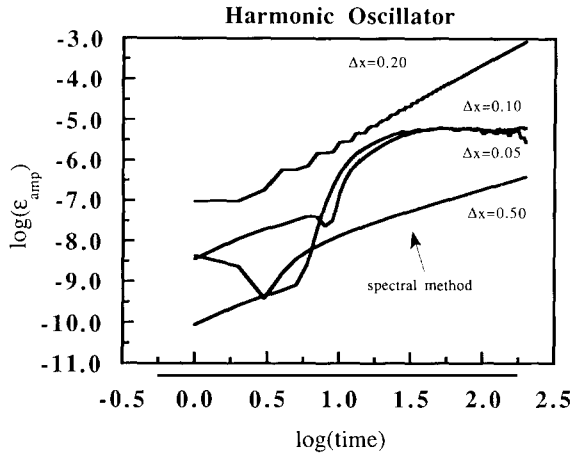

Fig. 3. The analogous results to fig. 1 for the harmonic oscillator potential are shown. Several different choices of grid spacing were used to demonstrate the error convergence of the differencing scheme.

reference wavefunction was a spectral representation with an error tolerance of 10^{-14}. The two smaller spacings yield adequate error control though markedly inferior to the spectral method. The phase error comparison in fig. 4 shows the same trend as that expected from the free particle case – the error accumulates primarily in the phase. All of these runs had purely real initial conditions ($p_0 = 0$).

Table 3
Morse potential numerical parameters (atomic units)

$N_{grid} = 512$	$x_0 = 14.0$	$\alpha = 1.0144$
$\Delta x = 0.10$	$\sigma = 1.0$	mass = 911.4
$\Delta t = 0.08$	$p_0 = -1.0, -10.0$	$D_0 = 0.1744$
		$r_e = -3.0$

The third and final test was chosen to mimic a typical heavy particle scattering event. A particle with the reduced mass of the hydrogen molecule was scattered from a Morse potential, $V(x) = D_0(e^{-2\alpha(r-r_e)} - 2e^{-\alpha(r-r_e)})$. The same form of the initial wavefunction was assumed as that given in eq. (9). The specific parameters used are listed in table 3. The initial wavefunction was positioned in the asymptotic region and given an initial component in the direction of the well. The "exact" wavefunction used for the comparisons in this case was calculated as before using the spectral method with Chebyshev expansion with an extremely small error tolerance, 10^{-14}. As before, the differencing method and spectral methods were applied with the same Chebyshev error tolerances, 10^{-8}.

Figures 5, 6, and 7 depict the results of this calculation. Figure 5 is a plot of the logarithmic amplitude error and fig. 6 is the analogous plot for the phase error as a function of time for two differencing calculations with different initial

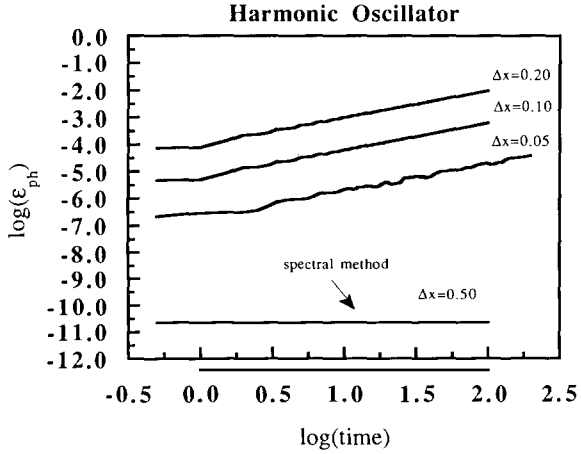

Fig. 4. The analogous results to fig. 2 for the harmonic oscillator potential are shown. The phase error again dominates the overall calculational error.

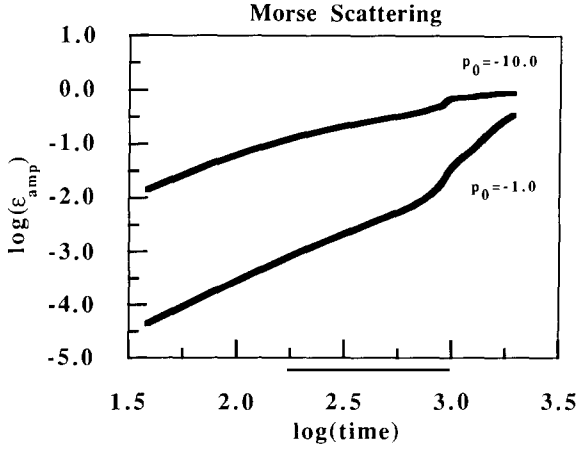

Fig. 5. The overlap amplitude error for two differencing solutions with different initial conditions for the Morse potential scattering The choices were $p_0 = -1.0, -10.0$ and $\sigma = 0.25$.

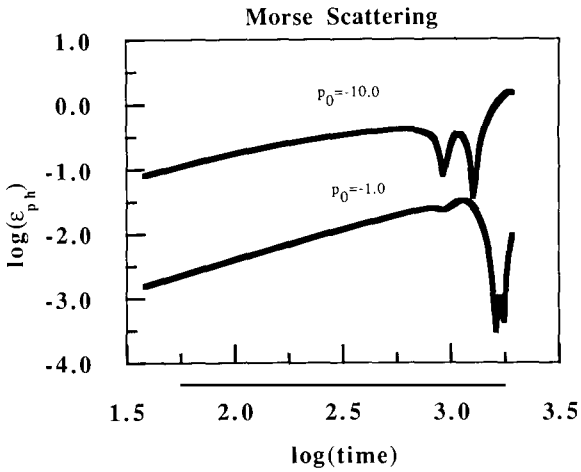

Fig. 6. The analogous results to fig. 5 for the phase error. The large error oscillations begin as reflection from the repulsive part of the potential grows.

wavepacket conditions. The errors are defined as in the previous cases. An additional comparison of the $p_0 = -1.0$ runs using the spectral and differencing methods is plotted in fig. 7. The amplitude and phase errors are plotted together in this figure. In all cases the trend observed previously holds – the differencing method is of much lower accuracy and efficiency than the spectral method

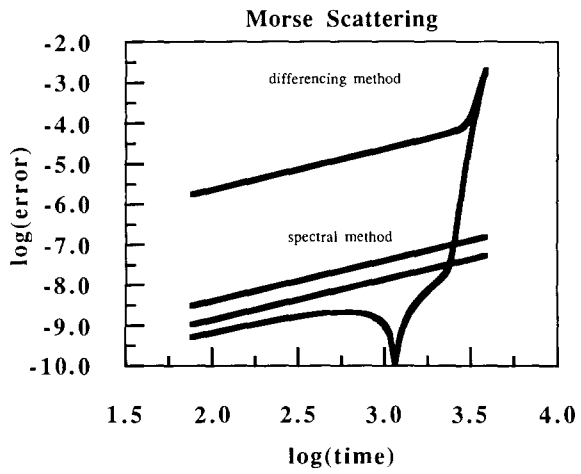

Fig. 7. The amplitude and phase error comparisons for the differencing and spectral methods with $p_0 = -1.0$ and $\sigma = 1.0$. The error in the amplitude of the wavefunction from the differencing method grows markedly once the particle reflects from the repulsive wall.

with a disproportionately large error in the phase. Once the particle enters the well and starts to interfere with itself, the accuracy of the differencing scheme is dramatically reduced.

4. Discussion

Two general conclusions follow from these simple tests. First, the Chebyshev expansion can be profitably used with a differencing scheme for the spatial derivatives. The low-order accuracy of the spatial approximation becomes the limiting factor in the error accumulation during time evolution, but large time steps are indeed possible. If the grid representation is adequate then the results obtained will be reliable to the error in the spatial derivatives with larger error in the wavefunction's phase than in its amplitude. The second salient feature demonstrated in these calculations is the relative inefficiency of the differencing method compared with the spectral decomposition in generating an accurate time-dependent wavefunction. An adequate spatial representation will be significantly more costly in terms of memory requirements *and* computing time for a differencing method. The general conclusion remains though – a low-order algorithm can be stably used with the Chebyshev expansion method.

Indeed, a recent two-dimensional model calculation of the photodissociation of the carbon dioxide molecule [6] displays the general features noted in the one-dimensional cases. On the other hand, the results of these calculations indicate that errors in the wavefunction itself might not necessarily translate into errors in the transition probabilities. A comparison of the time-dependent correlation functions from the spectral method calculation (solid line) and the differencing scheme (dotted line) is plotted in fig. 8. These results were obtained with the same grid spacing and time step. The peaks corresponding to recursions in the overlap are slightly lower and slightly delayed compared with those from the spectral method. This observation is consistent with the expectation that the higher-velocity components of the wavepacket will be inadequately sampled by the differencing scheme. The Fourier transform of this

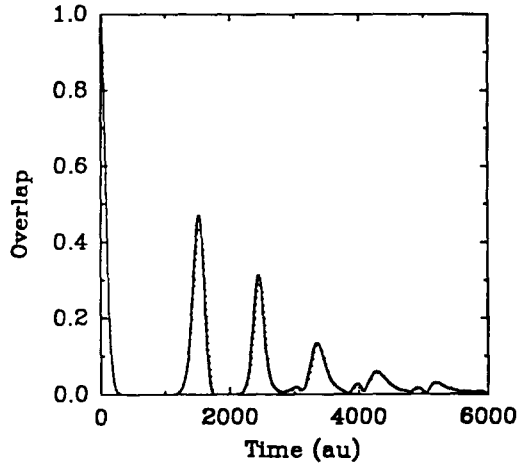

Fig. 8. The time-dependent correlation function, $\langle\phi(0)|\phi(t)\rangle$, for collinear CO_2 photodissociation. The solid line is the spectral method result and the dotted line is the differencing result. The overlap function was multiplied by 10 for times greater than 1000 atomic time units for clarity.

correlation function is proportional to the absorption lineshape. A comparison of the predicted absorption lineshape for the two calculations is given in fig. 9. The only significant errors in the differencing result occur near the resonances on the high-energy side of the peak. The dynamics of the dissociation process are very complex, as is obvious from the complicated structure in the lineshape; nonetheless, these features are reproduced by the differencing method. It should be noted that these results agree quantitatively with time-independent (R-matrix propagation) calculations for this system [7].

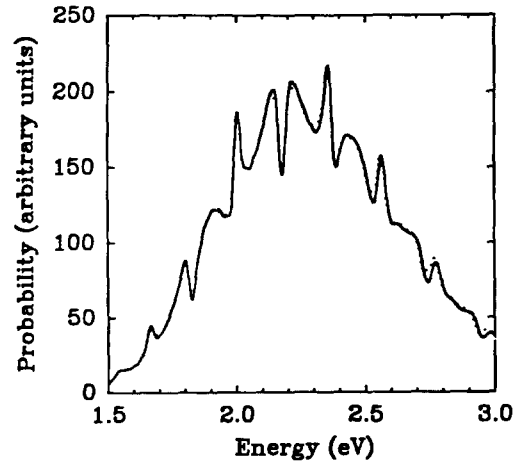

Fig. 9. The absorption lineshape corresponding to the correlation functions shown in fig. 8 (the temporal Fourier transform of the overlap).

A significant reduction of the computation time for these calculations by a factor of 12 was obtained by using the Chebyshev expansion method to increase the time step over that possible with a Crank–Nicolson propagation. Also, this calculation was a factor of four to five faster than the corresponding spectral method with maximum error of a few per cent. Further calculations revealed that the spectral method could not be used with a smaller grid than that for the differencing method.

Although the differencing approximation is not generally as accurate or efficient as the spectral representation, it should be emphasized that a simple low-order differencing method will be faster than a corresponding spectral calculation. If the desired quantities are intrinsically averaged, such as the autocorrelation functions in photodissociation for example, then a differencing method might be of sufficient accuracy to be the method of choice. Additionally, simple spectral methods are relatively inflexible with respect to boundary conditions since they rely on the band-limited nature of the represented function for their accuracy. In this case, a differencing method could again be a superior computational choice. Multigrid techniques are an obvious extension of this reasoning; physical problems with greatly different length scales can be readily addressed using finite differences since the boundary matching is relatively straightforward.

Acknowledgements

Work at the Lawrence Livermore National Laboratory is performed under the auspices of the US Department of Energy, administered by the University of California under Contract No. W-7405-Eng-48.

References

[1] E.A. McCullough and R.E. Wyatt, J. Chem. Phys. 51 (1969) 1253; J. Chem Phys. 54 (1971) 3592.
[2] M.D. Feit and J.A. Fleck Jr., Appl. Opt. 17 (1978) 3990.
M.D. Feit, J.A. Fleck Jr., and A. Steiger, J. Comput. Phys. 47 (1982) 412.
[3] D. Kosloff and R. Kosloff, J. Comput. Phys. 52 (1983) 35.
R. Kosloff and D. Kosloff, J. Chem. Phys. 79 (1983) 1823.
[4] H. Tal-Ezer and R. Kosloff, J. Chem. Phys. 81 (1984) 3967.
[5] K.C. Kulander, Phys. Rev. A 35 (1987) 445; 36 (1987) 2726.
J. Javanainen, J.H. Eberly and Q. Su, Phys. Rev. A 38 (1988) 3430.
[6] K.C. Kulander, C. Cerjan and A.E. Orel, J. Chem. Phys., in press.
[7] K.C. Kulander and J.C. Light, J. Chem. Phys. 73 (1980) 4337.